

Report to the 1964  
Dubna Conference

CERN/TC/PHYSICS 64-19  
2.6.1964

Not for Publication

THE ANNIHILATIONS OF 3.0 GEV/C ANTIPROTONS INTO K'S AND  $\pi$ 'S

B.R. French, J.B. Kinson, V. Šimák<sup>\*</sup>,

CERN, Geneva,

J. Badier, M. Bazin, A. Rougé,

Ecole Polytechnique, Paris,

and

P. Grieve

Imperial College, London.

-----

\* On leave from Physics Institute of Academy of Sciences, Prague.

1) Introduction

The Saclay 81cm hydrogen bubble chamber was exposed to a separated beam of antiprotons produced from an internal target in the CERN proton synchrotron. A total of 120,000 photographs were taken of  $0.8 \times 10^6$  antiprotons of 3.0 GeV/c momentum. From  $\delta$ -ray counting and total cross-section measurements the contamination of the beam has been estimated to be about 12%  $\mu$ s and 2% ns. The primary momentum spread was  $\pm 1.5\%$ . Results on hyperon-antihyperon production have been published previously<sup>(1)</sup>. We now discuss annihilations into  $K\bar{K}$  and  $n$  pions, where  $n$  is 1 to 5.

2) Cross-sections

The film was scanned for events in which one or two  $K^0$  decays were associated with an interaction giving 0, 2 or 4 charged tracks. From two independent scans, the overall efficiency for these types of event is estimated to be 97%. Approximately 1100 events at 3.0 GeV/c were measured by semi-automatic measuring machines, and their geometry and kinematics have been computed using the THRESH-GRIND system of programmes.

About 400 events were rejected as having more than one missing neutral particle, mainly events with 0 or 2 charged tracks. Of the remaining 700 events approximately 10% were not measurable or did not give a good geometrical reconstruction after several remeasurements. Events were classified into the reactions shown in Table I on the basis of the  $\chi^2$  calculated by the kinematics fitting programme. When several interpretations were possible, ionization measurements were made, thus reducing the number of ambiguous events to less than 20%.

The numbers of unique fit events used in the graphs are indicated in Table I. Of these about 60% depend on ionization measurements. The partial cross-sections shown in Table I have been corrected for scanning losses and unseen decays. Ambiguous and non-measurable events have been included in proportion to the well-fitted events.

### 3) Production of $K^*$ , $\rho$ and $\omega$

Only events with 4, 5 or 6 particles in the final state have sufficiently good statistics for a detailed study of resonance production to be worthwhile. For events with a charged K the third component of isotopic spin ( $T_z$ ) is known unambiguously for all combinations of particles, so that these events have been studied in more detail than those with  $K^0\bar{K}^0$ . In most cases the percentage of a resonance has been determined by fitting to the experimental ideogram a curve consisting of Lorentz invariant phase space together with a Breit-Wigner with the known mass and width of the resonance.

#### a) Invariant mass distributions for $(K\pi)$ combinations

All  $(K\pi)$  combinations with  $T_z = 3/2$  give invariant mass distributions which are in agreement with phase space. For  $T_z = 1/2$   $(K\pi)$  combinations the amount  $K^*$  production are shown in Table II for different reactions. The percentage of  $K^*$  production is defined as the number of  $(K\pi)$  combinations above phase space per 100 events. Figure 1 shows the invariant mass distributions for 4, 5 and 6-body events with a charged K. In the case of the 4-body events an enhancement is observed at a mass of 1400 MeV (2.5 standard deviations).

#### b) Invariant mass distributions for $(\pi\pi)$ combinations

The mass distribution for  $(\pi^+\pi^-)$  combinations in  $K^0\bar{K}^0\pi^+\pi^-$  final states (Figure 2a) gives some indication of  $\rho$  production, in the percentage given in Table II. There is also evidence for  $f^0$  production of approximately 15%.

For 5-body events the  $(\pi^+\pi^-)$  distribution (Figure 2b) shows the  $\rho^0$  and a smaller peak at 570 MeV. From the corresponding ideogram we estimate 40% of  $\rho$  production and  $20 \pm 10\%$  production of mass 570 MeV with a width of 40 MeV. Although of little significance as a single observation, we note that a similar peak with this mass and width has been observed by Ferbel et al.<sup>(2)</sup> and Lander et al.<sup>(3)</sup>.

Figure 2c shows all  $(\pi\pi)^+$  combinations for 6-body events with a charged K, and Figure 2d indicates those events which have no  $(\pi^+\pi^-\pi^0)$  mass in the  $\omega$  region (740-820 MeV). It can be seen that the  $\rho$  production becomes more significant when the background is reduced in this way.

### c) Invariant mass distributions for $(\pi\pi)$ combinations

For 5 and 6-body reactions, combinations with charge 1 or 2 give reasonable agreement with phase space (modified to include  $\rho$  production in the amounts given in the previous section). Also, the  $\pi^+\pi^-\pi^0$  masses from the final state  $K^0\bar{K}^0\pi^+\pi^-\pi^0$  show no significant  $\omega$  production. However, the reaction  $K^0K^{\pm}\pi^{\mp}\pi^+\pi^-\pi^0$  gives a clear  $\omega$  peak. The curve shown in Figure 3 represents phase space modified in accordance with the observed amount of  $\rho$  production (50%) and 25% of  $\omega$  production per event. The shaded histogram in Figure 3 is for those events which do not contain a  $(\pi\pi)^{+-0}$  mass in the  $\rho$  region (675-825 MeV). We estimate that the production of  $\omega$  in the final state  $K^0K^{\pm}\pi^{\mp}\pi^+\pi^-\pi^0$  is  $25 \pm 5\%$ .

### d) Associated production of resonances

From the amounts of  $K^*$ ,  $\rho$  and  $\omega$  production indicated above, it appears that the average number of resonances per event is approximately one or more for 5 and 6-body events with  $K^{\pm}$ . We have therefore studied the associated production of these resonances.

Five-body  $K^{\pm}$  events were selected which have a  $(K\pi)$  mass in the  $K^*_{888}$  region (830-945 MeV). For these events other possible  $(K\pi)$  combinations with  $T_Z = 1/2$  are shown in Figure 4a. From this we estimate that  $20 \pm 5\%$  of the events contain  $K^*+K^*$  (after corrections for  $K^*$  which are outside the selected region, and for the background which has been included). Similarly, the production of  $K^*+\rho$  is  $10 \pm 15\%$  in these events.

For 6-body  $K^{\pm}$  events, those with a  $(\pi^+\pi^-\pi^0)$  mass in the  $\omega$  region were selected, and the  $\omega+K^*$  production is estimated to be  $7 \pm 6\%$ . For these events the background included when considering the  $K^*$  and  $\rho$  regions is large. However, we observe no  $\rho+\rho$  production, and  $K^*+K^*$  is less than 10%. From these percentages and those for  $K^*$ ,  $\rho$  and  $\omega$  production, we estimate that  $20 \pm 20\%$  of the events will contain  $K^*+\rho$ . This agrees with the distribution of  $(K\pi)$  mass for events containing a  $\rho$  (Figure 4b).

### 4) Other possible resonances

In addition to the mass distributions studied above, we have plotted masses for all combinations of 2, 3 or 4 particles (including  $K^*$ ,  $\rho$  and  $\omega$ ). From these we observe two further possible resonances, which we shall now discuss.

a) KK $\pi$  at 1410 MeV

The invariant mass distribution for  $(K_1^0 K_1^+ \pi^-)$  is shown in Figure 5a for the 5-body final state  $K^0 K_1^+ \pi^- \pi^+ \pi^-$ . This shows some enhancement (2.5 S.D.) in the region of 1410 MeV, as observed previously by Armenteros et al.<sup>(4)</sup> We observe no departure from phase space for  $(K_1^0 K_1^0 \pi^\pm)$  masses in the final state  $K_1^0 K_1^0 \pi^+ \pi^- \pi^0$ , but the statistics are insufficient to draw any conclusions concerning the quantum numbers of the KK $\pi$  state.

Figure 5b shows the  $(K^* K)$  mass distribution for events in which one  $K\pi$  ( $T_z = 1/2$ ) combination has a mass in the interval 830 to 945 MeV; the peak at 1410 MeV is then more evident. We do not observe any accumulation of events in the  $K_{888}^*$  interference region of the Dalitz plot for the decay of this object. In addition, events which have no  $\rho$  have been selected, and the background is then further reduced. For 6-body events there is less evidence for any KK $\pi$  peak.

b) K $\pi\pi$  at 1270 MeV

For the 5-body events the  $(K\pi\pi)$  mass distributions show no significant deviations from phase space. The distributions for  $(K\pi\pi)$  are shown in Figure 6 for 6-body events with a charge K. Since we have 8 possible combinations with  $T_z = 1/2$  and 4 with  $T_z = 3/2$ , any resonance in this system would need to be strongly produced in order to be observed. Therefore, we have selected events with a  $K_{888}^*$  and studied the  $(K^* \pi)$  mass distributions, which are shown as shaded histograms in Figure 6. In Figure 6a we observe a  $K^* \pi$  peak at about 1270 MeV for  $T_z = 3/2$ ; it is more difficult to draw any conclusions for  $T_z = 1/2$  because of the larger background.

The  $(K\rho)$   $T_z = 3/2$  distribution is shown as a shaded histogram in Figure 7a, and this also provides some evidence for an excess of events above phase space in the same mass region. The larger histogram in Figure 7a is the sum of  $(K^* \pi)$  and  $(K\rho)$  with  $T_z = 3/2$ , and it shows a 4 standard deviation peak at about 1270 MeV.

To determine the mass and width of this enhancement, we show in Figure 7b a Gaussian ideogram of mass for  $(K^* \pi)$  with  $T_z = 3/2$  calculated using estimated errors of 14 MeV on the masses. Lorentz invariant phase space modified by a Breit-Wigner resonance was fitted to this ideogram, and from the best fit we obtain a mass of  $1270 \pm 20$  MeV and a width of  $60 \pm 30$  MeV. This should be compared with the results obtained by Armenteros et al.<sup>(5)</sup>, who find a resonance

with a mass of  $1230 \pm 10$  MeV and a width of  $80 \pm 10$  MeV in the  $T_z = 1/2$  combination  $K_1^0 \pi^+ \pi^-$ .

5) Angular distributions

In order to study the mechanism for antiproton annihilation in flight we have plotted angular distributions for particles and resonances (Figure 8).

The general characteristics of these distributions can be qualitatively understood in terms of a fermion exchange model for high energy annihilations of antiprotons (as suggested by Gribov<sup>(6)</sup> and Pilkuhn<sup>(7)</sup>), viz:-

- a) the  $K^- (K^+)$  angular distribution differs from the  $\pi^- (\pi^+)$  distribution in that the latter is symmetric about  $\cos \theta^* = 0$ , whereas the former is asymmetric with the  $K^- (K^+)$  going preferentially forward (backward) in the C.M.S.;
- b) the  $\bar{K}^0 (K^0)$  angular distribution is similar to the  $K^- (K^+)$  distribution;
- c) the K distributions are more peaked toward  $\cos \theta = \pm 1$  than the  $\pi$ 's;
- d) for the 5-body event the  $K^*$ 's are more peaked toward  $\cos \theta^* = \pm 1$  than the K's.

We acknowledge the assistance of the CERN proton synchrotron staff, members of the CERN T.C. Division who built the separated beam, and the crew of the 81cm Saclay bubble chamber. The CERN group would like to thank Mr. W. Tejessy for help in the computations.

Figure Captions

- Fig. 1 Distributions of invariant mass for all  $(K\pi)$  combinations with  $T_Z = \pm 1/2$ , for (a) 4-body, (b) 5-body, (c) 6-body (for final states with a charged K).
- Fig. 2 Distribution of invariant mass for :  
 (a)  $(\pi^+\pi^-)$  combinations for  $K^0 K^0 \pi^+ \pi^-$  final states  
 (b)  $(\pi^+\pi^-)$  " "  $K^0 K^{\pm} \pi^{\mp} \pi^+ \pi^-$  " "  
 (c)  $(\pi^+\pi^-)$  and  $(\pi^{\pm}\pi^0)$  combinations for the  $K^0 K^{\pm} \pi^{\mp} \pi^+ \pi^- \pi^0$  final states  
 (d) " " " " " " " " " "  
 for events which do not contain a  $(\pi^+\pi^-\pi^0)$  mass in the  $\omega$  region.
- Fig. 3 Mass distributions for  $(\pi^+\pi^-\pi^0)$  combinations from the final state  $K^0 K^{\pm} \pi^{\mp} \pi^+ \pi^- \pi^0$ . The shaded histogram indicates events which contain no  $(\pi\pi)^{+-0}$  masses in the  $\rho$  region.
- Fig. 4 Mass distributions for :  
 (a)  $(K\pi)$  combinations with  $T_Z = \pm 1/2$  for  $K^0 K^{\pm} \pi^{\mp} \pi^+ \pi^-$  final states which contain another  $K^{*888}$   
 (b)  $(K\pi)$  combinations with  $T_Z = \pm 1/2$  for  $K^0 K^{\pm} \pi^{\mp} \pi^+ \pi^- \pi^0$  final states which contain a  $\rho$ .
- Fig. 5 Mass distributions for the  $K^0 K^{\pm} \pi^{\mp} \pi^+ \pi^-$  final states :  
 (a)  $(K^0 K^{\pm} \pi^{\mp})$  combinations with  $T_Z = 0$   
 (b)  $(K^{*888} K)$  " " "  
 (c)  $(K^{*888} K)$  " " " for events not containing a  $\rho$ .
- Fig. 6 Mass distributions for  $K^0 K^{\pm} \pi^{\mp} \pi^+ \pi^- \pi^0$  final states :  
 (a)  $(K\pi\pi)$  combinations with  $T_Z = \pm 1/2$ . The shaded histogram shows those combinations which contain a  $K^{*888}$ .  
 (b) The same as (a) for  $T_Z = \pm 3/2$  combinations.
- Fig. 7 Mass distributions for  $K^0 K^{\pm} \pi^{\mp} \pi^+ \pi^- \pi^0$  final states :  
 (a) The sum of  $(K^{*888}\pi)$  and  $(K\rho)$  combinations with  $T_Z = \pm 3/2$ ; the shaded area indicates  $(K\rho)$  combinations only.  
 (b) Ideogram for  $(K^{*888}\pi)$  combinations with  $T_Z = \pm 3/2$ . The curve shows phase space modified with a Breit-Wigner resonance curve with mass 1270 MeV and width 60 MeV.

Fig. 8 Centre of mass angular distributions for  $\pi^-, K^-, \bar{K}^0, \bar{K}^{*888}$  (plus reflected  $\pi^+, K^+, K^0, K^{*888}$ ).

References

- (1) B. Musgrave et al., CERN/TC/PHYSICS 64-1 (to be published)  
Preliminary results were given by Armenteros et al., Proc. Int. Conf. on High Energy Physics, CERN, p.236 (1962)
- (2) T. Ferbal et al., Bull.Am.Phys.Soc., 9, p.22 (1964)  
A more recent preprint by the same authors explains this effect as a statistical fluctuation.
- (3) R.L. Lander et al., Preprint (March 1964)
- (4) R. Armenteros et al., Sienna Conf. Proc., p.287 (1963)
- (5) R. Armenteros et al., Phys.Lett., 9, p.207 (1964)
- (6) V.N. Gribov and D.V. Volkov, Proc. Int. Conf. on High Energy Physics, CERN, p.552 (1962)
- (7) H. Pilkuhn, Arkiv för Fysik, 23, p.471 (1962)



Table I

Partial cross-sections for  $\bar{p}p \rightarrow K\bar{K}+n\pi$

n	Reaction	No. of events	$\sigma$ ( $\mu\text{b}$ )
1	$K_1^0 K_1^+ \pi^- \bar{\pi}^0$	10	$17 \pm 5$
	$K_1^0 K_1^0 \pi^0$	1	$0.5 \pm 0.5$
2	$K_1^0 K_1^\pm \pi^\mp \pi^0$	73	$272 \pm 32$
	$K_1^0 K_1^0 \pi^+ \pi^-$	35	$80 \pm 20$
3	$K_1^0 K_1^\pm \pi^\mp \pi^+ \pi^-$	137	$210 \pm 30$
	$K_1^0 K_1^0 \pi^+ \pi^- \pi^0$	63	$140 \pm 30$
4	$K_1^0 K_1^\pm \pi^\mp \pi^+ \pi^- \pi^0$	183	$275 \pm 37$
	$K_1^0 K_1^0 \pi^+ \pi^+ \pi^- \pi^-$	56	$90 \pm 25$
	$K_1^0 K_1^0 \pi^+ \pi^+ \pi^- \pi^-$	20	$52 \pm 15$
5	$K_1^0 K_1^0 \pi^+ \pi^+ \pi^- \pi^- \pi^0$	13	$30 \pm 12$
6	$K_1^0 K_1^0 \pi^+ \pi^+ \pi^- \pi^0 + \pi^0 \pi^0$	3	$5 \pm 3$

Table II

Production of  $K^*$  and  $\rho$

No. of particles in the final state	Reaction	No. of $(K\pi)$ combinations/ events	Percentage of $K^*$ production	No. of $(\pi\pi)$ combinations with charge 0 or 1	Percentage of $\rho$ production
4	$K_1^0 K_1^0 \pi^+ \pi^-$	4	$30 \pm 12$	1	$15 \pm 10$
4	$K_1^0 K_1^\pm \pi^\mp \pi^0$	4	$15 \pm 10$	1	$10 \pm 10$
5	$K_1^0 K_1^0 \pi^+ \pi^- \pi^0$	6	$50 \pm 20$	3	$40 \pm 20$
5	$K_1^0 K_1^\pm \pi^\mp \pi^+ \pi^-$	4 with $T_z = \pm 1/2$	$65 \pm 15$	2	$35 \pm 10$
6	$K_1^0 K_1^0 \pi^+ \pi^+ \pi^- \pi^-$	8	$50 \pm 30$	4	$30 \pm 20$
6	$K_1^0 K_1^\pm \pi^\mp \pi^+ \pi^- \pi^0$	6 with $T_z = \pm 1/2$	$60 \pm 10$	5	$50 \pm 20$

FIG. 1

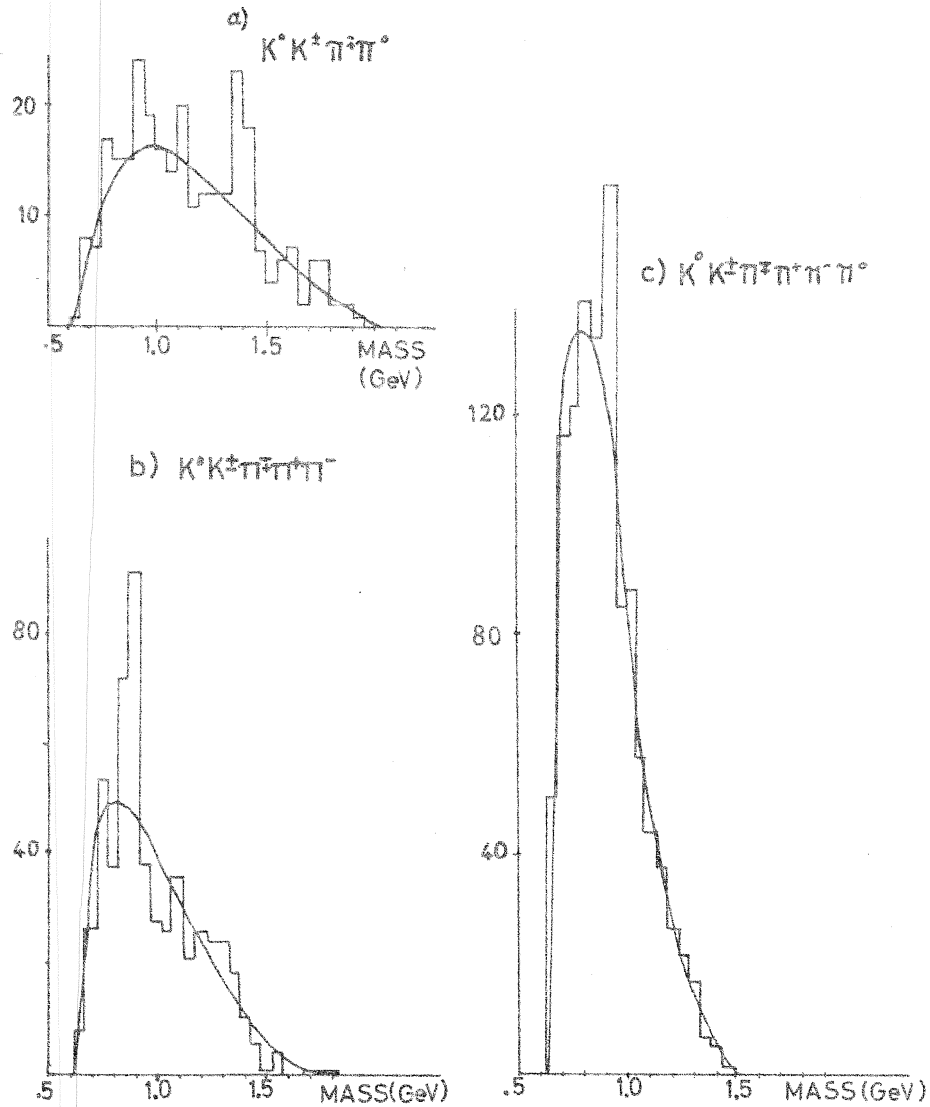
 $(K\pi) T_{\frac{1}{2}} = \frac{1}{2}$ 

FIG. 2

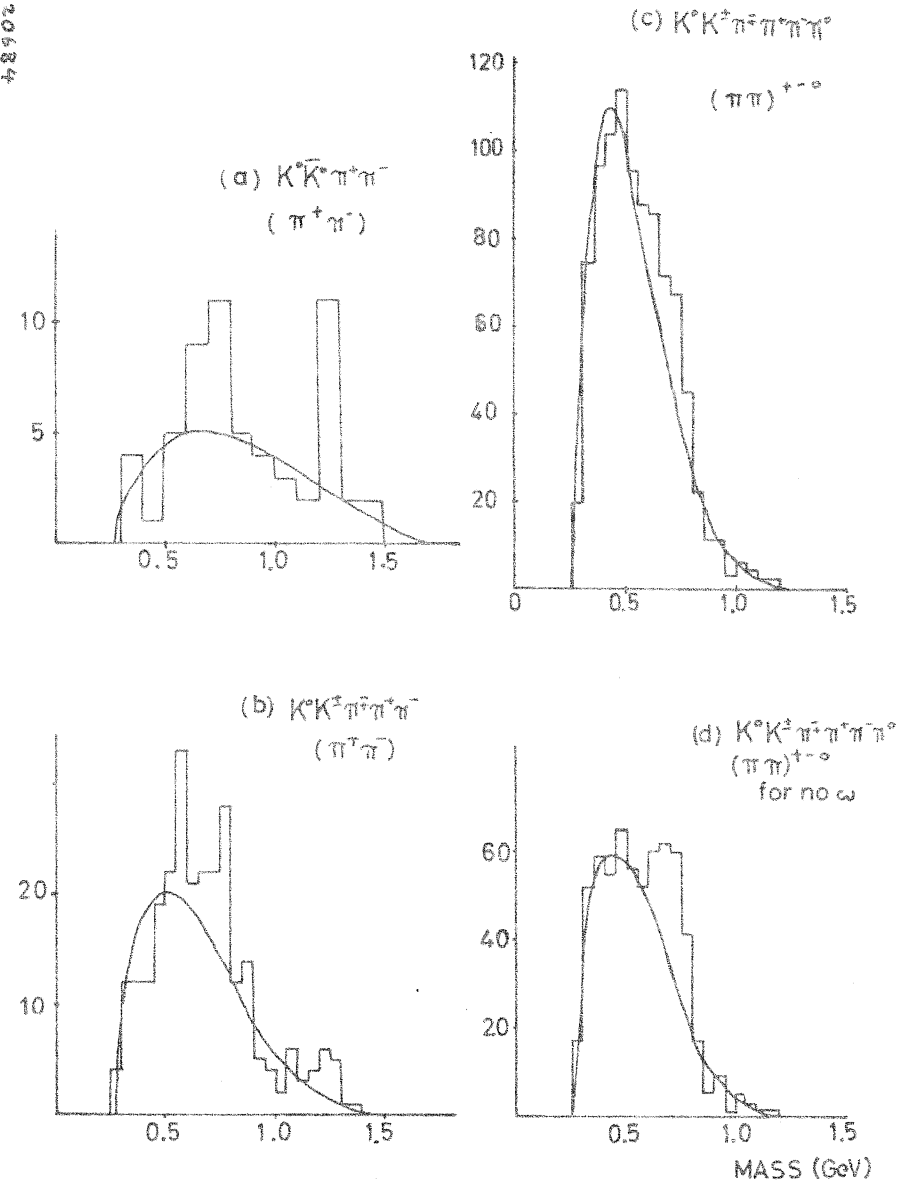


FIG. 3

$K^0 K^{\pm} \pi^{\mp} \pi^+ \pi^- \pi^0$

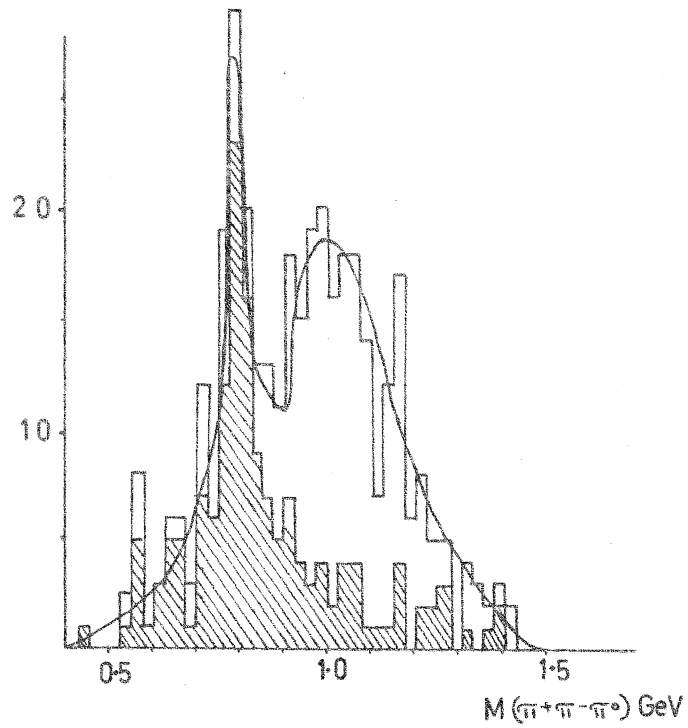
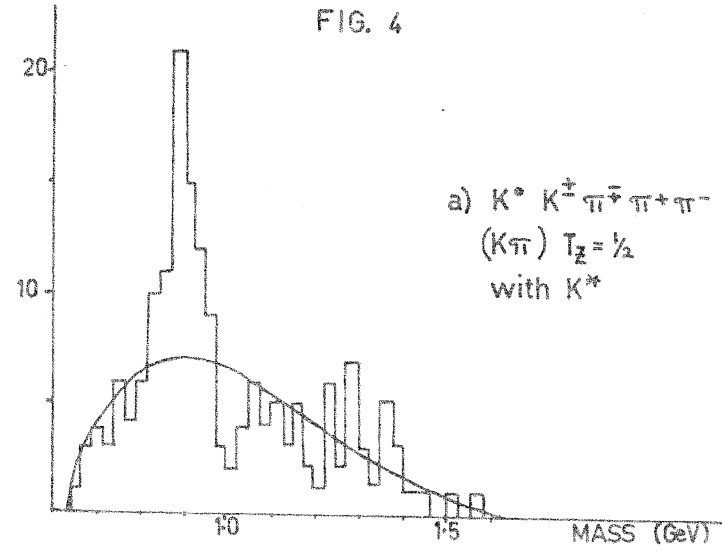


FIG. 4

a)  $K^0 K^{\pm} \pi^{\mp} \pi^+ \pi^-$   
 $(K\pi) T_Z = \frac{1}{2}$   
 with  $K^{*0}$



b)  $K^0 K^{\pm} \pi^{\mp} \pi^+ \pi^- \pi^0$   
 $(K\pi) T_Z = \frac{1}{2}$   
 with  $\rho$

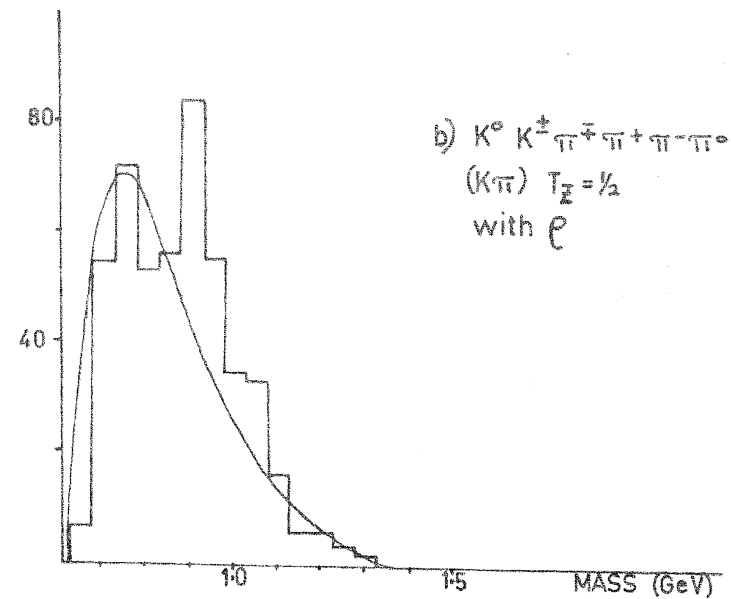


FIG. 5  
 $K^0 K^\pm \pi^\mp \pi^+ \pi^-$

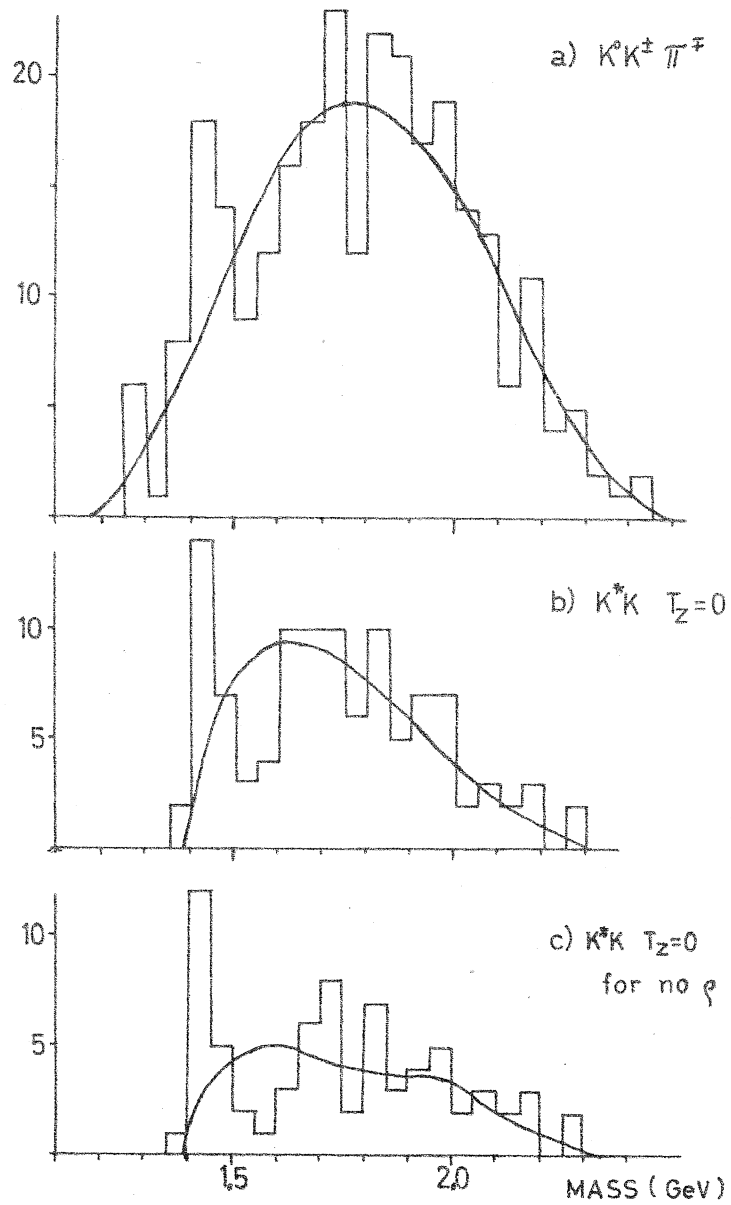


FIG. 6  
 $K^0 K^\pm \pi^\mp \pi^+ \pi^- \pi^0$

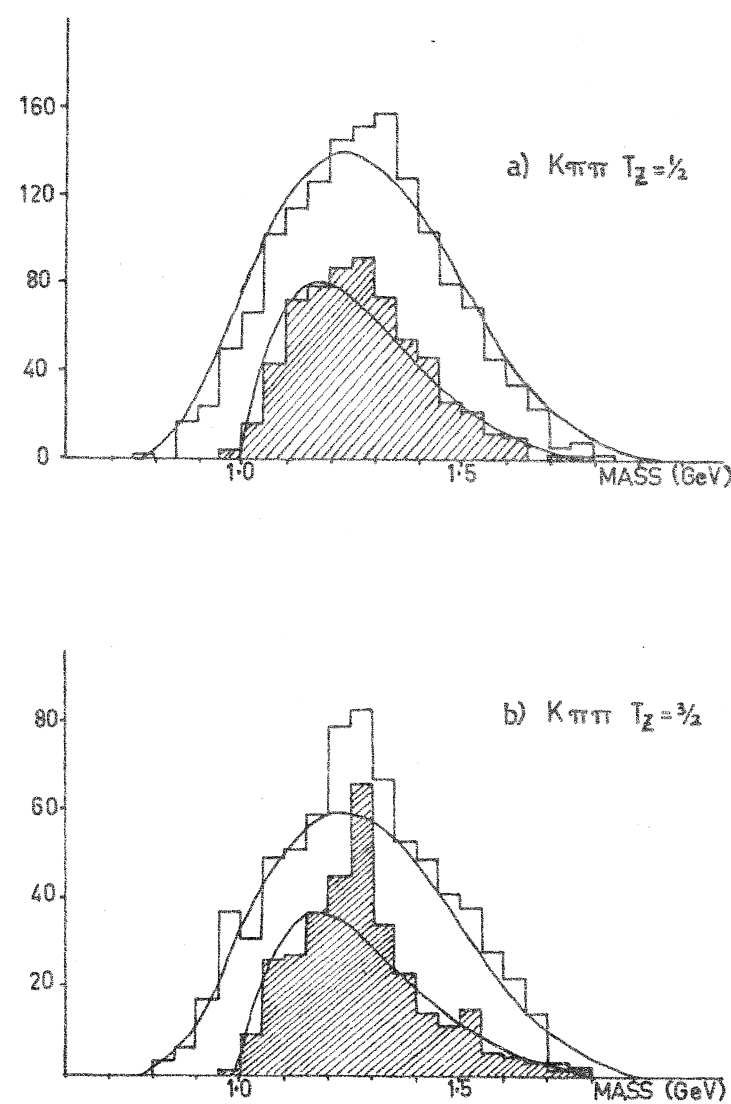


FIG. 7

$K^0 K^{\pm} \pi^{\mp} \pi^{\pm} \pi^{\mp} \pi^{\pm} \pi^{\pm}$

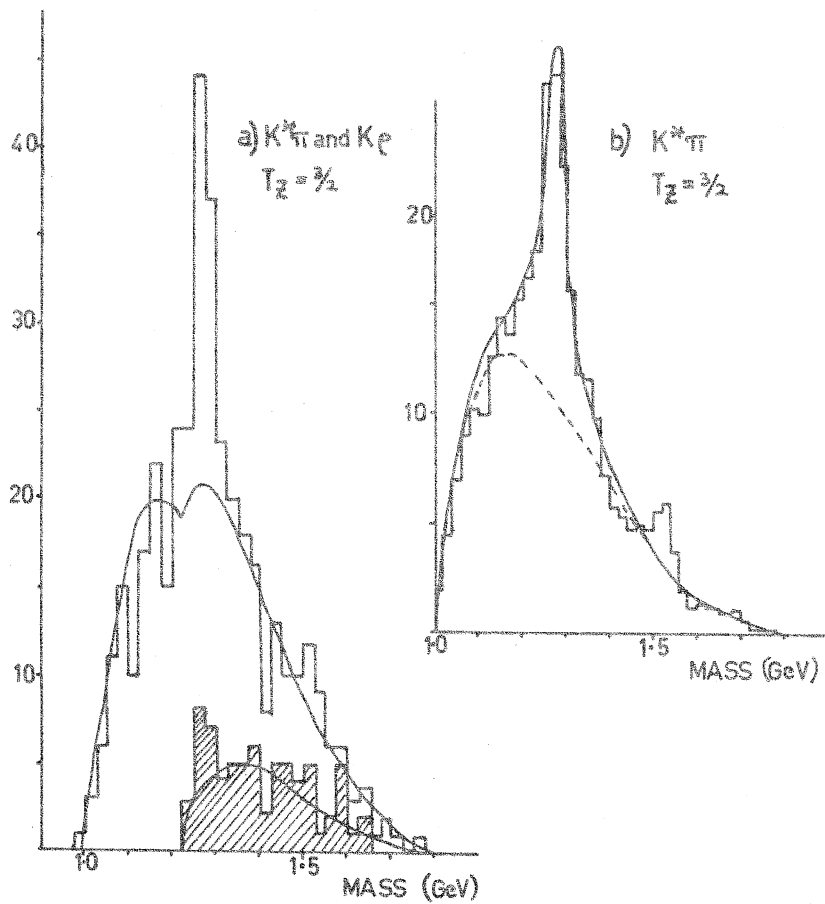


FIG. 8

